

Physiological consequences of height-related morphological variation in *Sequoia sempervirens* foliage

LUCY P. MULLIN,^{1,2} STEPHEN C. SILLETT,³ GEORGE W. KOCH,¹
KEVIN P. TU⁴ and MARIE E. ANTOINE⁵

¹ Biological Sciences and Merriam-Powell Center for Environmental Research, Northern Arizona University, Flagstaff, AZ 86011, USA

² Corresponding author (lucy.mullin@nau.edu)

³ Department of Forestry and Wildland Resources, Humboldt State University, Arcata, CA 95521, USA

⁴ Department of Integrative Biology, University of California, Berkeley, CA 94720, USA

⁵ Department of Biological Sciences, Humboldt State University, Arcata, CA 95521, USA

Received February 18, 2009; accepted May 2, 2009

Summary This study examined relationships between foliar morphology and gas exchange characteristics as they vary with height within and among crowns of *Sequoia sempervirens* D. Don trees ranging from 29 to 113 m in height. Shoot mass:area (SMA) ratio increased with height and was less responsive to changes in light availability as height increased, suggesting a transition from light to water relations as the primary determinant of morphology with increasing height. Mass-based rates of maximum photosynthesis ($A_{\max,m}$), standardized photosynthesis ($A_{\text{std},m}$) and internal CO₂ conductance ($g_{i,m}$) decreased with height and SMA, while the light compensation point, light saturation point, and mass and area-based rates of dark respiration (R_m) increased with height and SMA. Among foliage from different heights, much of the variation in standardized photosynthesis was explained by variation in g_i , consistent with increasing limitation of photosynthesis by internal conductance in foliage with higher SMA. The syndrome of lower internal and stomatal conductance to CO₂ and higher respiration may contribute to reductions in upper crown growth efficiency with increasing height in *S. sempervirens* trees.

Keywords: internal conductance, photosynthesis, respiration, tree height.

Introduction

Foliar morphology often varies within the crowns of forest trees, with values of common metrics (leaf mass:area, LMA or shoot mass:area, SMA) typically increasing with height. Some of this plasticity is a response to light level and appears to improve resource allocation for light harvesting (Givnish 1986, Leverenz 1996, Niinemets and Kull 1998, Niinemets

et al. 1998, Bond et al. 1999). Hydraulic constraints may also contribute to variation in foliar morphology, particularly in tall trees (Marshall and Monserud 2003, Koch et al. 2004, Woodruff et al. 2004, Ishii et al. 2008). As the vertical distance between roots and leaves lengthens, gravity and friction increase the hydrostatic and hydrodynamic components, respectively, of xylem tension (Zimmermann 1983). As a result, protoplasts at greater heights should experience reduced turgor pressure or require increased solute accumulation to drive water absorption for turgor maintenance. Estimates of declining turgor pressure with height suggest that osmotic adjustment is incomplete (Koch et al. 2004, Woodruff et al. 2004, Meinzer et al. 2008), and this may lead to reduced leaf expansion and increased LMA or SMA. Other factors such as reduced tracheid hydraulic conductivity (Domec et al. 2008) may further impact cellular water relations and contribute to reduced leaf expansion as trees approach apparent height limits.

If the structure of the foliage is constrained by height-related factors, physiological functions of foliage may be compromised in tall trees. Variation in LMA is often inversely correlated with leaf internal conductance to CO₂, g_i , the diffusive conductance from the substomatal chamber through intercellular airspaces, cell walls and the liquid phase of mesophyll cells to the sites of carboxylation within chloroplasts (Evans et al. 1986, Evans et al. 1994, Hanba et al. 1999, Warren et al. 2004, Warren 2008). Thus, the increase in LMA with height might limit leaf gas exchange by reducing g_i . Vertical trends of increasing foliar $\delta^{13}\text{C}$ in many tall-growing tree species (reviewed in Ryan et al. 2006) indicate that the total leaf conductance (stomatal, g_s plus g_i) limitation of photosynthesis generally increases with height. The extent to which reductions in g_i contribute to this height-related variation in foliar $\delta^{13}\text{C}$ is unclear. In Douglas-fir, g_i of lower and upper crown leaves did not

differ (Warren et al. 2003), but g_i of treetop foliage decreased with height (Woodruff et al. 2008), implying that lower g_i contributed to the observed declines in ambient photosynthesis with increasing tree height. So far, Douglas-fir is the only tall species for which g_i has been quantified across a height gradient.

Height-related variation in foliar morphology may also impact gas exchange by affecting the balance of photosynthesis and respiration. At the species level, high LMA or SMA is often associated with an increased proportion of non-photosynthetic tissue (Niinemets 1999, Reich et al. 1999), higher light compensation point (LCP) (Lewis et al. 2000), decreased mass-based photosynthesis (Koch et al. 2004, Ishii et al. 2008) and higher respiration relative to photosynthesis (Griffin et al. 2001, Tissue et al. 2002, Zha et al. 2002). Although numerous studies have documented lower photosynthesis in foliage from taller trees and a few have described reductions in crown growth efficiency with height (Ryan et al. 2006), it remains the extent to which changes in leaf structure, via effects on gas exchange characteristics and carbon balance, contribute to this pattern.

In *Sequoia sempervirens* D. Don (coast redwood, Cupressaceae) trees (hereafter redwood), foliar morphology ranges from bilaterally flattened shoots with leaves in a single plane in the lower crown to shoots near the treetop that have reduced, scale-like leaves arranged radially around the stem (Koch et al. 2004, Ishii et al. 2008). In the tallest redwoods, which are over 110 m in height and have crowns up to 80 m in depth, LMA varies nearly threefold, and both SMA and light-saturated photosynthesis vary fourfold along vertical gradients of light and water potential (Ishii et al. 2008). Within-crown variation in foliar $\delta^{13}\text{C}$ of these trees spans much of the range observed in C_3 species, with treetop values of -22‰ to -24‰ , indicative of strong limitation of CO_2 assimilation by CO_2 concentration (Koch et al. 2004). While field measurements document periods of lower stomatal conductance at the tops of taller compared to shorter redwoods (Sillett and Ambrose, unpublished data), it is unclear whether this is adequate to account for the observed variation in foliar $\delta^{13}\text{C}$ with height. Understanding how g_i varies with height and foliar morphology would help resolve the role of stomatal regulation and internal conductance in determining foliar $\delta^{13}\text{C}$. Laboratory measurements of gas exchange have documented a reduction in maximum photosynthetic rate (A_{max}) along a height gradient within tall redwood crowns (Koch et al. 2004, Ishii et al. 2008) and at the tops of redwoods of different heights (Ambrose et al. 2009), but relationships between internal conductance and foliar morphology have not been examined.

This study investigated the links between foliar morphology and components of photosynthetic and respiratory gas exchange along height and light availability gradients in redwood. We tested two primary hypotheses: (1) with increasing SMA, dark respiration rate (R_m) increases relative to maximum photosynthesis and (2) leaf internal conductance to CO_2 decreases as SMA increases.

Materials and methods

Study site

We selected 20 redwood trees for intensive study (Sillett et al., unpublished data). These trees occur on the north coast of California in Humboldt Redwoods State Park, an old-growth forest along the alluvial terraces of Bull Creek, a tributary of the Eel River (Van Pelt and Franklin 2000). This forest is located at 40.3° N and 124.0° W, between 30 and 50 m a.s.l., and has a mean annual temperature of 12.6°C and a mean annual precipitation of 1226 mm with $< 2\%$ occurring in the dry summer season (National Weather Service Data for Scotia, CA). The climate is coastal-Mediterranean with periods of fog during summer.

Sampling protocol

Five trees, whose tops were exposed to full sun, were chosen from each of the four height classes: 29–36, 68–75, 90–96 and 108–113 m (hereafter referred to as 30, 70, 90 and 110 m). Trees were nondestructively accessed using ropes and arborist-style climbing techniques (Jepson 2000). In October 2007, branches ~ 1 m in length and 1 cm in basal diameter were cut, wrapped in a plastic bag to reduce transpiration and transported to ground level where they were re-cut under water, removing 10–15 cm of length. In the laboratory, all branches were again re-cut under water, this time removing 2–5 cm. Before beginning gas exchange measurements, the cut branches were allowed to acclimate for 3–12 h. All gas exchange measurements were done within 36 h of removal from the tree. Because of the small size of individual redwood leaves and being closely appressed to the stem in upper crown foliage (Ishii et al. 2008), it was not possible to measure gas exchange using individual leaves. Instead, all gas exchange measurements were of shoots, defined here as one annual segment with all its leaves. Thus, foliage inside the gas exchange chamber included stem and leaf tissues.

To examine the relationships between shoot morphology and gas exchange parameters along the vertical, within-crown gradient, a branch was taken from within 5 m of the treetop, from the middle of the live crown, and from the base of the live crown in each of the tallest trees. To characterize the effects of height, with minimal variation in light, on foliar morphology and physiology, we sampled all 20 treetops (< 5 m from highest leaf). To compare treetop light levels, direct site factor (DSF), indirect site factor (ISF) and % canopy openness were quantified with WinSCANOPY from hemispherical photographs taken via a digital camera on a self-leveling mount (Version 2002a, Régent Instruments, Inc., Quebec, Canada).

Morphological measurements

Area and mass of shoot segments were measured to quantify foliar morphology. After gas exchange measurements, each shoot was digitally scanned (Epson America, Inc., Long Beach, CA) and then ImageJ (National Institute of Health,

Bethesda, MD) was used to calculate the projected shoot surface area (A_s) of the silhouette. Shoots were then dried at 60 °C for 48 h and weighed to the nearest 0.1 mg. Shoot dry mass (M_s) was divided by A_s to determine SMA. For each sample, morphological measurements were based only on the portion of the shoot used for gas exchange analysis.

Gas exchange measurements

Gas exchange was quantified with a LI-6400 portable photosynthesis system (Li-Cor, Lincoln, NE). For each branch, one terminal shoot was placed in the 2 × 3 cm standard leaf chamber equipped with a red-blue LED source (model 6400-02B). Preliminary tests with a second quartz-halogen light source illuminating the leaf from below (through a transparent chamber bottom) produced no increase in net CO₂ assimilation above that achieved with saturating light from the LED source alone, indicating that the internal reflection within the Li-Cor leaf chamber adequately illuminated the underside of the shoot. The seam between the top and bottom of the leaf chamber was sealed with putty to eliminate CO₂ leaks. For all measurements block temperature was set to 25 °C and leaf temperature was measured with a thermocouple in contact with the underside of the shoot. Leaf-to-air vapor pressure deficit was maintained between 1.4 and 2.0 kPa.

Light response curves Light response curves were used to estimate A_{\max} , R_m , light saturation point (LSP) and LCP for each shoot. The reference CO₂ was set to 400 μmol CO₂ mol⁻¹ and photosynthetic photon flux density (PPFD) varied from 0 to 2000 μmol photons m⁻² s⁻¹. To solve for A_{\max} , LSP and LCP, light curves were analysed using a program available from Li-Cor, Inc. (www.licor.com) based on the study of Norman and Arkebauer (1991). R_m was measured after 8 min of darkness. The high light (PPFD = 2000 μmol photons m⁻² s⁻¹) C_i values from all shoots were averaged to calculate the standardized C_i , which was then used with individual shoots' $A-C_i$ response to estimate the standardized maximum photosynthesis, A_{std} (see the following section).

$A-C_i$ response curves Our estimates of g_i and A_{std} in redwood foliage used $A-C_i$ rather than $A-C_c$ relationships. We recognize that $A-C_c$ curves are preferred for quantifying the biochemical differences underlying gas exchange parameters, but the C_c estimates that we obtained via indirect methods were inconsistent (Ethier and Livingston 2004, Sharkey et al. 2007). Internal conductance, g_i , was estimated from a method based on the difference between the chloroplastic and the intercellular photocompensation points (photocompensation point method, Peisker and Apel 2001). Here, g_i is defined as the total CO₂ conductance from the substomatal chamber through the intercellular airspaces, mesophyll cell wall and mesophyll cell cytoplasm to the chloroplast. The photocompensation point (Γ^*) is the CO₂ concentration at which photosynthetic CO₂ uptake is exactly compensated by photorespiratory CO₂ release (Sharkey et al. 2007). The intercellular CO₂ concentration

(C_i) is the substomatal chamber CO₂ concentration. The intercellular compensation point (C_i^*) is the C_i value at which the chloroplastic CO₂ concentration equals Γ^* . C_i^* is related to Γ^* by the mitochondrial respiration rate in the light (day respiration, R_d) and g_i (von Caemmerer and Evans 1991, Peisker and Apel 2001):

$$C_i^* = \Gamma^* - R_d/g_i. \quad (1)$$

To estimate g_i for each shoot, a partial $A-C_i$ curve was run at three different light levels (PPFD of 1000, 200 and 50 μmol photons m⁻² s⁻¹) for a total of three curves. Each curve was run at low reference CO₂ values of 250, 200, 100, 50 and 0 μmol CO₂ mol⁻¹, thereby producing only the linear portion. Lines generated at different light intensities for each shoot produced three intersection points. The ordinate of each intersection point is R_d , and the abscissa is C_i^* (Laisk 1977). Thus, each intersection yields a (C_i^* , R_d) coordinate set. Average C_i^* and R_d values determined from these three coordinate sets were used to estimate g_i . Γ^* was determined as the ordinate of a line fitted to a plot of these three (C_i^* , R_d) points. Using Γ^* , and average C_i^* and R_d values, g_i was calculated for each shoot (Warren et al. 2003):

$$g_i = R_d/(\Gamma^* - C_i^*). \quad (2)$$

For each shoot, an $A-C_i$ response curve was also run at PPFD = 1600 μmol m⁻² s⁻¹, with the reference CO₂ (μmol CO₂ mol⁻¹) set to the following sequence: 380, 275, 175, 100, 50, 380, 550, 700, 900, 1200, 1600 and 2000. Ordinary least-squares regression analysis including all the points of this $A-C_i$ curve was used to determine an equation for the best-fit line for each curve. The standard C_i value determined from the light response curves was then used with this equation to solve for A_{std} .

Statistical analysis

Ordinary least-squares regression analysis was used to examine changes in dependent variables in relation to height using JMP (SAS Institute, Cary, NC). Regression was performed along the within-tree gradient and across treetops of different heights, and adjusted R^2 values are reported. JMP was also used for one-way ANOVA and orthogonal contrast post hoc tests to determine significant differences among groups. To test the assumption of homogeneous variance, Levine and Bartlett tests were used. When this assumption was violated, Welch tests were used to note the significant differences among groups.

For summary of terms and definitions used in this study refer to Appendix (Table A1).

Results

Treetop light environment

Treetop light levels were lower in shortest trees than the other height classes (Table 1). Canopy openness, DSF

and ISF all varied significantly among height classes, with values generally being lower in 30 m treetops and varying little among 70, 90 and 110 m treetops.

Shoot morphology

Shoot mass:area correlated positively with height within crowns (Table 2, $R^2 = 0.70$, $P = 6.2E-07$). Among treetops, SMA also correlated positively with height (Table 3, $R^2 = 0.78$, $P = 1.6E-07$). The SMA of 30 m treetops was lower than all other height classes (Figure 1), and SMA of 70 m treetops differed from all other height classes.

Light response curves

Maximum photosynthesis $A_{\max,m}$ correlated negatively with height within crowns (Table 2, $R^2 = 0.34$,

$P = 0.013$), and $A_{\max,m}$ was lower in treetop shoots than in mid-crown and base-of-live-crown shoots (Figure 2D). As SMA increased, $A_{\max,a}$ increased (Figure 3A, $R^2 = 0.32$, $P = 0.016$) and $A_{\max,m}$ decreased (Figure 3D, $R^2 = 0.48$, $P = 0.003$). Among treetops, $A_{\max,m}$ correlated negatively with height (Table 3, $R^2 = 0.73$, $P = 1.1E-08$), and $A_{\max,m}$ was highest in the shortest trees (Figure 2D). As SMA increased among treetops, $A_{\max,m}$ decreased (Figure 3D, $R^2 = 0.68$, $P = 4.7E-06$).

Mitochondrial respiration $R_{m,a}$ ($R^2 = 0.70$, $P = 6.5E-05$) and $R_{m,m}$ ($R^2 = 0.58$, $P = 0.0006$) both correlated positively with height within crowns (Figure 2B and E). Respiration rates were significantly higher in treetop shoots compared to the mid-crown and base-of-live-crown shoots (Table 2).

Table 1. Summary of treetop light environment for each height class. Values are mean \pm 1 SE ($n = 5$). Mean values with same superscript do not differ significantly ($P < 0.05$).

Characteristic	30 m	70 m	90 m	110 m	<i>P</i>
Canopy openness (%)	50.1 ^a \pm 2.4	74.4 ^b \pm 2.6	83.0 ^c \pm 0.6	88.7 ^c \pm 1.0	< 0.0001
DSF	88.5 ^a \pm 3.8	96.2 ^{ab} \pm 1.3	99.9 ^b \pm 0.0	100.0 ^b \pm 0.0	0.0179
ISF	76.8 ^a \pm 2.5	93.6 ^b \pm 1.7	98.2 ^b \pm 0.1	99.1 ^b \pm 0.1	0.0001

Table 2. Summary of physiological and morphological characteristics of foliage within tall tree crowns. Values are mean \pm 1 SE ($n = 5$). Mean values with same superscript do not differ significantly ($P < 0.01$).

Characteristic	Base-of-live-crown	Mid-crown	Treetop	<i>P</i>
$A_{\max,a}$ ($\mu\text{mol CO}_2 \text{ m}^{-2} \text{ s}^{-1}$)	8.57 ^a \pm 1.67	14.04 ^a \pm 2.38	14.12 ^a \pm 1.27	0.0873
$A_{\max,m}$ ($\text{nmol CO}_2 \text{ g}^{-1} \text{ s}^{-1}$)	54.81 ^a \pm 9.24	52.70 ^a \pm 2.4	24.17 ^b \pm 1.71	0.0036
$A_{\text{std},a}$ ($\mu\text{mol CO}_2 \text{ m}^{-2} \text{ s}^{-1}$)	7.96 ^a \pm 2.01	12.33 ^a \pm 1.55	9.97 ^a \pm 1.35	0.2173
$A_{\text{std},m}$ ($\text{nmol CO}_2 \text{ g}^{-1} \text{ s}^{-1}$)	51.01 ^a \pm 7.20	47.27 ^a \pm 2.58	19.72 ^b \pm 4.78	0.0014
$R_{m,a}$ ($\mu\text{mol CO}_2 \text{ m}^{-2} \text{ s}^{-1}$)	0.64 ^a \pm 0.12	1.27 ^a \pm 0.26	5.91 ^b \pm 0.45	< 0.0001
$R_{m,m}$ ($\text{nmol CO}_2 \text{ g}^{-1} \text{ s}^{-1}$)	3.97 ^a \pm 0.45	4.77 ^a \pm 0.67	10.33 ^b \pm 1.14	0.0002
LCP ($\mu\text{mol photons m}^{-2} \text{ s}^{-1}$)	14 ^a \pm 2	20 ^a \pm 3	103 ^b \pm 20	< 0.0001
LSP ($\mu\text{mol photons m}^{-2} \text{ s}^{-1}$)	938 ^a \pm 143	1018 ^a \pm 127	1506 ^b \pm 68	0.0111
$g_{i,a}$ ($\text{mol CO}_2 \text{ m}^{-2} \text{ s}^{-1} \text{ bar}^{-1}$)	0.034 ^a \pm 0.004	0.041 ^a \pm 0.004	0.036 ^a \pm 0.003	0.1282
$g_{i,m}$ ($\text{nmol CO}_2 \text{ g}^{-1} \text{ s}^{-1} \text{ bar}^{-1}$)	0.19 ^a \pm 0.01	0.16 ^a \pm 0.01	0.06 ^b \pm 0.01	0.0003
SMA (g m^{-2})	172 ^a \pm 13	351 ^b \pm 38	633 ^c \pm 27	< 0.0001
LMA (g m^{-2})	125 ^a \pm 7	154 ^b \pm 7	202 ^c \pm 6	< 0.0001

Table 3. Summary of physiological and morphological characteristics for treetop foliage of each height class. Values are mean \pm 1 SE ($n = 5$). Mean values with same superscript do not differ significantly ($P < 0.05$).

Characteristic	30 m	70 m	90 m	110 m	<i>P</i>
$A_{\max,a}$ ($\mu\text{mol CO}_2 \text{ m}^{-2} \text{ s}^{-1}$)	17.21 ^a \pm 2.16	19.62 ^a \pm 2.66	19.98 ^a \pm 2.61	14.12 ^a \pm 1.27	0.2658
$A_{\max,m}$ ($\text{nmol CO}_2 \text{ g}^{-1} \text{ s}^{-1}$)	74.91 ^a \pm 8.88	46.06 ^b \pm 6.00	34.82 ^b \pm 4.07	24.17 ^b \pm 1.71	0.0395
$A_{\text{std},a}$ ($\mu\text{mol CO}_2 \text{ m}^{-2} \text{ s}^{-1}$)	14.17 ^a \pm 1.88	15.95 ^a \pm 2.37	14.8 ^a \pm 1.49	9.97 ^a \pm 1.35	0.1938
$A_{\text{std},m}$ ($\text{nmol CO}_2 \text{ g}^{-1} \text{ s}^{-1}$)	62.24 ^a \pm 9.74	37.59 ^{ab} \pm 6.28	25.86 ^b \pm 2.31	19.72 ^b \pm 3.83	0.0009
$R_{m,a}$ ($\mu\text{mol CO}_2 \text{ m}^{-2} \text{ s}^{-1}$)	1.59 ^a \pm 0.18	2.50 ^b \pm 0.21	4.89 ^c \pm 0.29	5.91 ^d \pm 0.45	< 0.0001
$R_{m,m}$ ($\text{nmol CO}_2 \text{ g}^{-1} \text{ s}^{-1}$)	6.80 ^{ab} \pm 0.56	6.03 ^a \pm 0.89	8.56 ^{bc} \pm 0.48	10.33 ^c \pm 1.14	0.0097
LCP ($\mu\text{mol photons m}^{-2} \text{ s}^{-1}$)	23 ^a \pm 3	40 ^a \pm 9	70 ^b \pm 3	103 ^c \pm 20	< 0.0001
LSP ($\mu\text{mol photons m}^{-2} \text{ s}^{-1}$)	1292 ^a \pm 91	1377 ^a \pm 94	1512 ^a \pm 59	1506 ^a \pm 68	0.1903
$g_{i,a}$ ($\text{mol CO}_2 \text{ m}^{-2} \text{ s}^{-1} \text{ bar}^{-1}$)	0.046 ^a \pm 0.006	0.045 ^a \pm 0.006	0.045 ^a \pm 0.001	0.036 ^a \pm 0.003	0.315
$g_{i,m}$ ($\text{nmol CO}_2 \text{ g}^{-1} \text{ s}^{-1} \text{ bar}^{-1}$)	0.20 ^a \pm 0.03	0.11 ^b \pm 0.02	0.08 ^b \pm 0.00	0.06 ^b \pm 0.01	0.0149
SMA (g m^{-2})	275 ^a \pm 33	463 ^b \pm 13	578 ^c \pm 8	633 ^c \pm 27	< 0.0001
LMA (g m^{-2})	149 ^a \pm 8	184 ^b \pm 5	201 ^c \pm 1	202 ^c \pm 6	< 0.0001

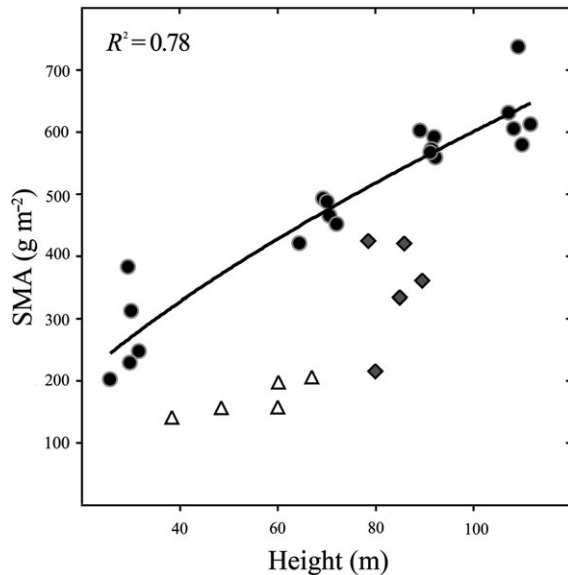


Figure 1. SMA ratio (g m^{-2}) correlated positively with height in redwoods. Regression line fitted to data for treetop foliage (black circles) of four height classes. Grey diamonds and open triangles are mid-crown and base-of-live-crown foliage, respectively, of tallest height class.

As SMA increased within crowns, $R_{m,a}$ ($R^2 = 0.82$, $P = 2.4\text{E}-06$) and $R_{m,m}$ ($R^2 = 0.45$, $P = 0.004$) both increased (Figure 3B and E). Among treetops, R_m differed significantly among all height classes (Table 3), and the increase in R_m with height was most strongly expressed on an area basis (Figure 2B, $R^2 = 0.79$, $P = 8.7\text{E}-08$). As SMA increased among treetops, $R_{m,a}$ increased (Figure 3B, $R^2 = 0.60$, $P = 3.4\text{E}-05$).

Light saturation point The LSP correlated positively with height within crowns (Figure 4A, $R^2 = 0.48$, $P = 0.003$) and was higher in treetop shoots than in mid-crown and base-of-live-crown shoots (Table 2). The LSP also increased with SMA within crowns (Figure 4C, $R^2 = 0.66$, $P = 0.0002$).

Light compensation point The LCP correlated positively with height within crowns (Figure 4B, $R^2 = 0.61$, $P = 0.0004$), and this was higher in treetop shoots compared to mid-crown and base-of-live-crown shoots (Table 2). The LCP also increased with SMA within crowns (Figure 4D, $R^2 = 0.62$, $P = 0.0003$), and this LCP correlated positively with height among treetops (Figure 4B, $R^2 = 0.69$, $P = 3.6\text{E}-08$) such that LCP in 90 m treetops was higher than that in 30 and 70 m treetops, and LCP of 110 m treetops was higher than that in all other height classes (Table 3). The LCP also increased with SMA among treetops (Figure 4D, $R^2 = 0.36$, $P = 0.003$).

A-C_i response curves

Internal conductance Within crowns, $g_{i,m}$ correlated negatively with height (Figure 2F, $R^2 = 0.52$, $P = 0.002$) and was significantly lower at the treetop than elsewhere in the crown (Table 2). As SMA increased in the tallest trees, $g_{i,m}$ decreased ($R^2 = 0.72$, $P = 3.9\text{E}-05$, Figure 3F). Among treetops, $g_{i,m}$ correlated negatively with height (Figure 2F, $R^2 = 0.67$, $P = 6.4\text{E}-08$) and was significantly higher in the shortest trees than in all other height classes (Table 3). As SMA increased among treetops, $g_{i,m}$ decreased (Figure 3F, $R^2 = 0.65$, $P = 1.1\text{E}-05$).

Assimilation at a standardized intercellular CO_2 concentration The average C_i value for all shoots at high light was $247 (\mu\text{mol CO}_2 \text{ mol}^{-1})$. At this standard C_i , assimilation per unit area ($A_{\text{std},a}$) within crowns and among treetops was weakly correlated with height and SMA. On a mass basis, assimilation ($A_{\text{std},m}$) at this standard C_i was more strongly correlated with height and SMA than with $A_{\text{max},m}$ derived from light response curves. Within crowns, $A_{\text{std},m}$ correlated negatively with height (Figure 5A, $R^2 = 0.41$, $P = 0.006$) and was significantly lower at the treetop (Table 2). As SMA increased within crowns and among treetops, $A_{\text{std},m}$ also decreased (Figure 5B, $R^2 = 0.64$ and 0.84 , $P = 0.0002$ and $6.4\text{E}-06$ for within crowns and among treetops, respectively). $A_{\text{std},m}$ was positively correlated with $g_{i,m}$ within crowns (Figure 5C, $R^2 = 0.89$, $P = 1.1\text{E}-07$). Among treetops, $A_{\text{std},m}$ correlated negatively with height (Figure 5A, $R^2 = 0.64$, $P = 1.2\text{E}-05$), was significantly higher in the shortest trees (Table 3), and was positively correlated with $g_{i,m}$ (Figure 5C, $R^2 = 0.84$, $P = 9.9\text{E}-09$).

Discussion

Most previous investigations of relationships between light, height and foliar morphology have been conducted on trees less than 65 m tall (e.g., Bauerle et al. 1999, McDowell et al. 2002, Phillips et al. 2003). It has been suggested that in redwoods the dominant mechanism controlling shoot morphology shifts from light to water potential around 70 m (Ishii et al. 2008). Thus, in tall redwoods where light is a confounding factor up to ~ 70 m (Ishii et al. 2008), study trees below this height may not be suitable for making inferences about distinguishing the effects of light availability versus water potential unless light levels and leaf water potentials are measured and the appropriate analyses are conducted to parse out the respective effects of these two factors. In the tallest redwoods, light availability increases exponentially while water potential decreases linearly along a vertical gradient of 110 m or more (Jennings 2002, Koch et al. 2004, Ishii et al. 2008).

Using this extreme height gradient, our experimental design attempted to separate effects of light and hydrostatic

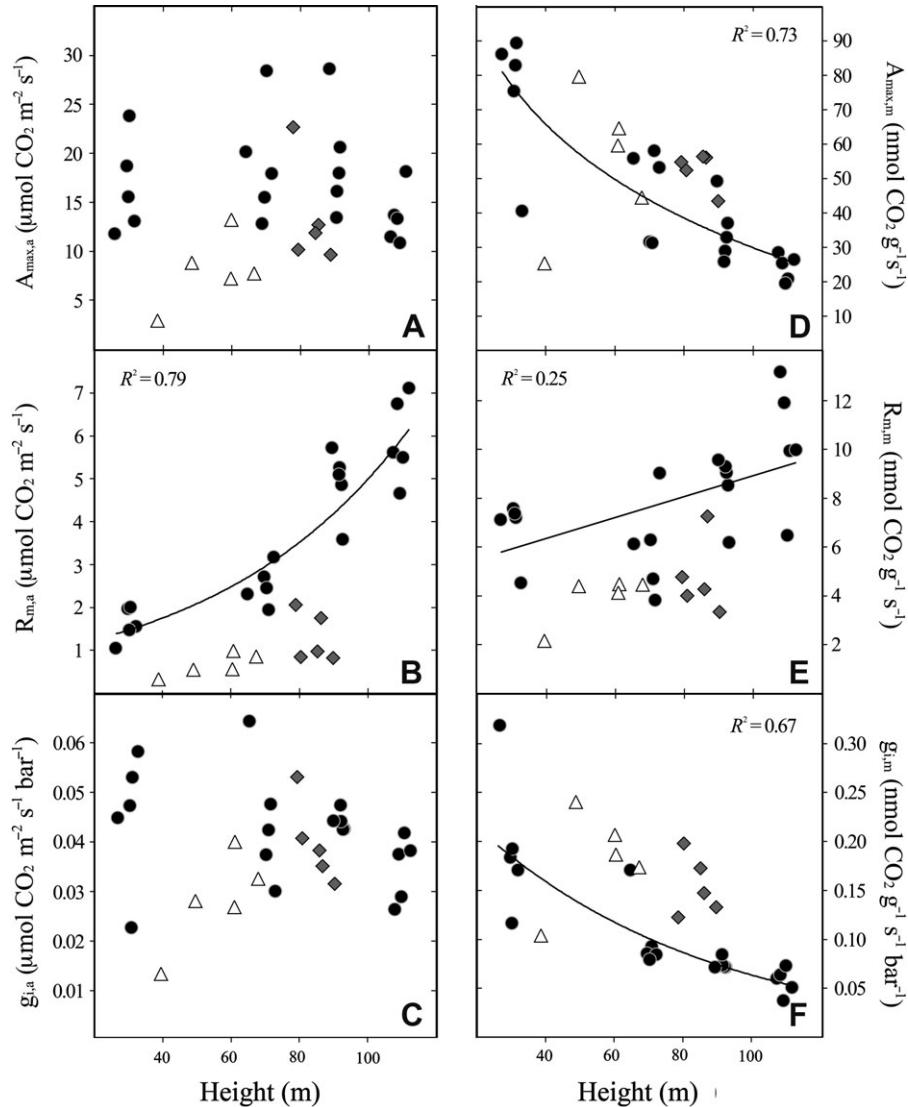


Figure 2. Variation with height and light availability in gas exchange characteristics of redwood foliage. (A) Light-saturated photosynthetic rate per unit area ($\mu\text{mol CO}_2 \text{ m}^{-2} \text{ s}^{-1}$) did not vary with height. (B) Dark mitochondrial respiration rate per unit area ($\mu\text{mol CO}_2 \text{ m}^{-2} \text{ s}^{-1}$) increased exponentially with height. (C) Internal conductance per unit area ($\mu\text{mol CO}_2 \text{ m}^{-2} \text{ s}^{-1} \text{ bar}^{-1}$) did not vary with height or light. (D) Light-saturated photosynthetic rate per unit mass ($\text{nmol CO}_2 \text{ g}^{-1} \text{ s}^{-1}$) correlated negatively with height. (E) Dark mitochondrial respiration rate per unit mass ($\text{nmol CO}_2 \text{ g}^{-1} \text{ s}^{-1}$) correlated positively with height. (F) Internal conductance per unit mass ($\text{nmol CO}_2 \text{ g}^{-1} \text{ s}^{-1} \text{ bar}^{-1}$) correlated negatively with height. Regression lines fitted to data from 20 treetops. Gas exchange measurements were done under relaxed water potential. Different symbols consistent for A–F: black circles, treetops; grey diamonds, mid-crown of tallest height class; and open triangles, base-of-live-crown of tallest height class.

tension on foliar morphology. The relative importance of these two factors changes with height. In the shaded lower crown where light interception is a high priority, hydrostatic tension does not hinder leaf expansion and we see low SMA shoot morphologies (Figure 1). However, in the mid-crown where light is still below saturation, hydrostatic tension might inhibit foliar expansion and light interception (Ishii et al. 2008). A hydraulic component to this gradient in SMA was confirmed by a linear increase in SMA among treetops from different height classes (Figure 1). Although our 30 m treetops were more shaded than taller treetops, mor-

phological differences between 70 m and even taller treetops existed at nearly uniform high light levels (Table 1) demonstrating that hydrostatic tension affects foliar morphology.

While its morphological effects are obvious and macroscopic, the cellular consequences of hydrostatic tension are more difficult to discern. In the absence of osmotic compensation, hydrostatic tension decreases water potential so that, ultimately, leaf turgor decreases with height (Koch et al. 2004, Woodruff et al. 2004, Meinzer et al. 2008). In redwoods, this decrease in turgor has been measured as 0.006 MPa m^{-1} (Koch et al. 2004). Thus, the observed

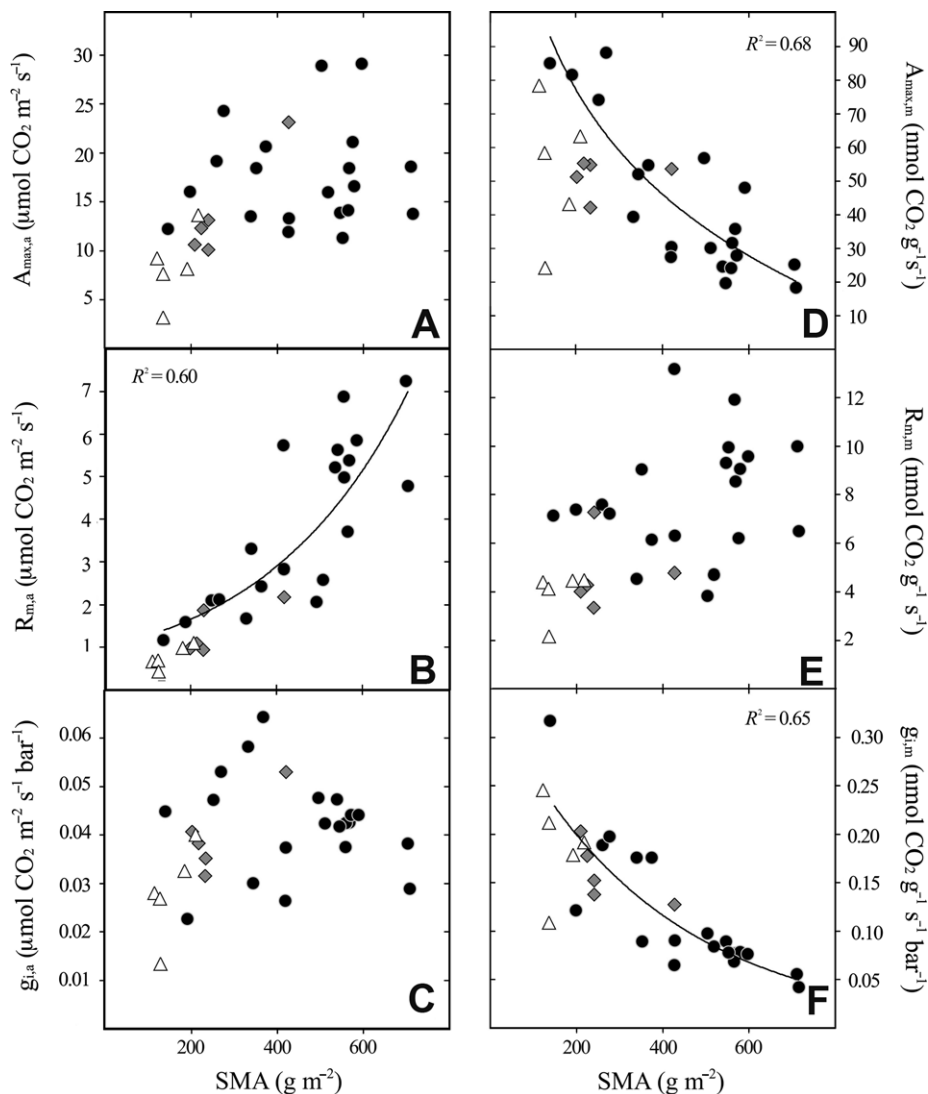


Figure 3. Variation in gas exchange features in relationship to SMA of redwood foliage. (A) Light-saturated photosynthetic rate per unit area ($\mu\text{mol CO}_2 \text{ m}^{-2} \text{ s}^{-1}$) did not vary with SMA. (B) Dark mitochondrial respiration rate per unit area ($\mu\text{mol CO}_2 \text{ m}^{-2} \text{ s}^{-1}$) increased exponentially with SMA. (C) Internal conductance per unit area ($\mu\text{mol CO}_2 \text{ m}^{-2} \text{ s}^{-1} \text{ bar}^{-1}$) did not vary with SMA. (D) Light-saturated photosynthetic rate per unit mass ($\text{nmol CO}_2 \text{ g}^{-1} \text{ s}^{-1}$) decreased with SMA. (E) Dark mitochondrial respiration rate per unit mass ($\text{nmol CO}_2 \text{ g}^{-1} \text{ s}^{-1}$) did not vary with SMA. (F) Internal conductance per unit mass ($\text{nmol CO}_2 \text{ g}^{-1} \text{ s}^{-1} \text{ bar}^{-1}$) decreased with SMA. Regression lines fitted to data from 20 treetops. Gas exchange measurements were done under relaxed water potential. Different symbols consistent for A–F: black circles, treetops; grey diamonds, mid-crown of tallest height class; and open triangles, base-of-live-crown of tallest height class.

positive correlation between hydrostatic tension and SMA (Ishii et al. 2002, 2008, Jennings 2002, Koch et al. 2004) is likely due to decreasing turgor. At the anatomical level, high SMA is associated with increased mesophyll density and thickness, and decreased intercellular airspace relative to the amount of mesophyll area (mesoporosity, Hanba et al. 1999, Niinemets 1999, Ishii et al. 2002, Jennings 2002, Oldham 2008). These morphological and anatomical changes occurring along the vertical gradient have photosynthetic consequences (Niinemets 1999, Koch et al. 2004). Results of this study suggest that hydrostatic tension contributes to structural changes at the shoot level that

indirectly reduce net photosynthesis via increased respiration rates and decreased internal CO_2 conductance.

Anatomical properties associated with high SMA also influence rates of mitochondrial respiration. As surface area for light interception decreases and non-photosynthetic mass increases, respiration rates rise along the vertical gradient (Figure 2B, see also Griffin et al. 2001, Tissue et al. 2002, Zha et al. 2002). The positive correlation between R_m and SMA both within crowns and among treetops of different heights (Figure 3B) suggests that foliage with dense tissue may be more costly to produce and to maintain than foliage with less dense tissue. To protect against UV-B damage,

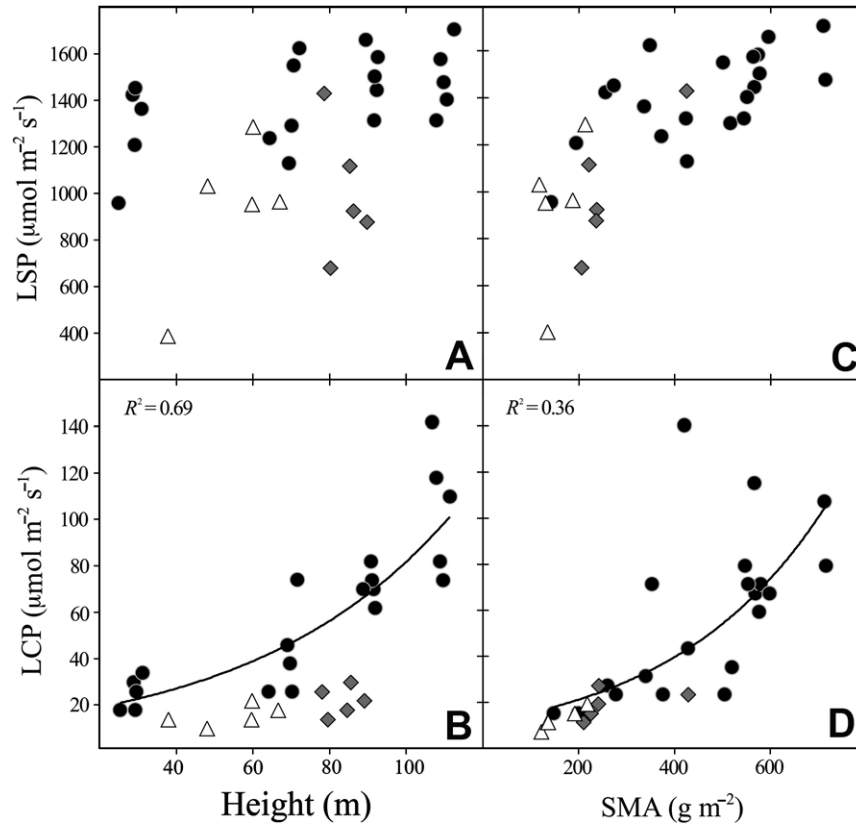


Figure 4. Variation with height and SMA in light saturation and compensation points. (A) LSP ($\mu\text{mol photons m}^{-2} \text{s}^{-1}$) measured at 95% of $A_{\text{max,a}}$ did not vary with height. (B) LCP ($\mu\text{mol photons m}^{-2} \text{s}^{-1}$) increased exponentially with height and light availability. (C) LSP increased with SMA within tall trees. (D) LCP increased exponentially with SMA. Regression lines fitted to data from 20 treetops. Photosynthetic measurements were done under relaxed water potential. Different symbols are consistent for A–D: black circles, treetops; grey diamonds, mid-crown of tallest height class; and open triangles, base-of-live-crown of tallest height class.

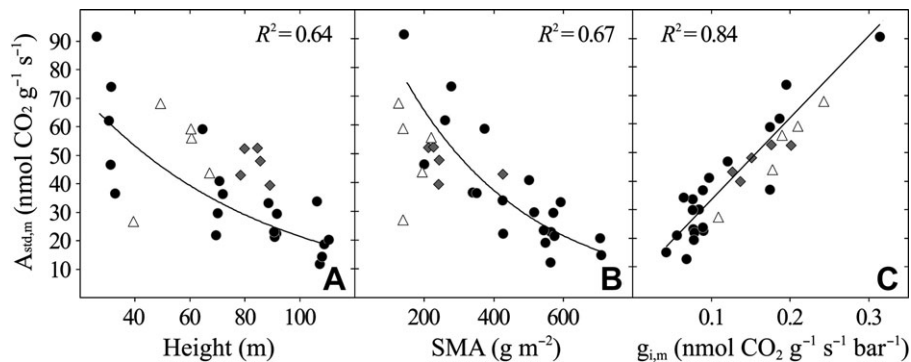


Figure 5. Variations of photosynthetic rate per unit mass ($\text{nmol CO}_2 \text{g}^{-1} \text{s}^{-1}$) at a standardized C_i value of $247 \mu\text{mol CO}_2 \text{mol}^{-1}$. (A) Photosynthetic rate per unit mass correlated negatively with height (m). (B) Photosynthetic rate per unit mass decreased with SMA (g m^{-2}). (C) Photosynthetic rate per unit mass increased with mass-based internal conductance ($\text{nmol CO}_2 \text{g}^{-1} \text{s}^{-1} \text{bar}^{-1}$). Regression lines fitted to data from 20 treetops. Different symbols consistent for A–C: black circles, treetops; grey diamonds, mid-crown of tallest height class; and open triangles, base-of-live-crown of tallest height class.

high-irradiance foliage is associated with high concentrations of soluble phenolics such as flavonoids (Li et al. 1993). This investment in secondary metabolites could contribute to the high mitochondrial respiration rates observed in high-SMA foliage (Poorter et al. 2006, 2009). These trends in soluble phenolics and mitochondrial respiration with

irradiance, as well as our observation of higher SMA in treetop foliage than non-treetop foliage at similar heights, suggest that high irradiance also contributes to high SMA.

In addition to increasing respiratory costs, anatomical properties associated with high SMA influence CO_2 diffusion within the leaf. The consistent decrease in $g_{i,m}$ with

SMA (Figure 3F) suggests that dense tissue is less conductive to CO₂ diffusion. This negative correlation between tissue density and CO₂ conductance has been demonstrated or proposed in other studies (Syvertsen et al. 1995, Niinemets 1999, Ishii et al. 2008). As mesophyll density and thickness increase and mesoporosity decreases, CO₂ moves more slowly from the substomatal chamber to carboxylation sites (Teeri et al. 1981, Syvertsen et al. 1995). Distances between substomatal chambers and sites of carboxylation consist of a gaseous phase through the intercellular airspaces (g_{ias}) and a liquid phase through mesophyll cytoplasm (g_{liq}). The CO₂ diffusion coefficient in the liquid phase is much slower than in air, thereby making the g_{liq} component of internal conductance more constraining (Nobel 1983, Maxwell et al. 1997). Coupling of increased thickness and decreased mesoporosity increases both path length and the liquid phase of g_i . Because tissue density is partly dependent on hydrostatic tension, height-related declines in turgor likely increase tissue density and thereby decrease $g_{i,m}$ (Koch et al. 2004, Ishii et al. 2008, Meinzer et al. 2008). Water stress also affects g_i , which contributes to the observed decrease in $g_{i,m}$ along the hydrostatic gradient (Warren et al. 2004, Flexas et al. 2008).

Stomatal frequency and distribution of palisade mesophyll are two other important leaf properties that change with SMA. High SMA is generally associated with increased stomatal frequency, abaxial and adaxial stomatal distribution (amphistomatous), and upper and lower palisade levels (Zimmermann 1971, Jennings 2002). This bi-layered distribution of both stomata and palisade tissue should increase g_i by shortening the internal path length for diffusion (Mott et al. 1982). However, because g_{liq} is the most limiting component of g_i , the conductive benefit of a decreased path length in amphistomatous leaves is overpowered by an increased liquid phase associated with increased cell density (Hanba et al. 1999, Gorton et al. 2003).

Importance of the observed correlations between height and $g_{i,m}$ is challenged by some recent literature. For example, internal CO₂ conductance has a considerable amount of plasticity and can respond rapidly to environmental and internal factors via activity of aquaporins and carbonic anhydrases (Flexas et al. 2008). Although the plastic nature of g_i complicates interpretation of our observations, all measurements in this study were done under standardized laboratory conditions. Our g_i results likely reflect real differences caused by internal factors related to morphology rather than responses to environmental variation.

Height-related changes in morphology and anatomy influence photosynthetic potential by affecting respiration rate and CO₂ conductance. The values and relationships reported here are based on gas exchange measurements done under relaxed water potential and therefore are free from stomatal limitation. In situ consequences of hydraulic limitation are more pronounced than those reported here due to reductions in stomatal conductance as height increases (Ryan and Yoder 1997, Warren et al. 2003, Koch et al. 2004). Both

stomatal and non-stomatal limitations constrain photosynthesis. Non-stomatal limitations include morphological, anatomical, biochemical and physiological shifts that occur along the hydrostatic gradient. These limitations likely contribute to the decreased $A_{max,m}$ observed with height in tall redwood trees (Jones and Slatyer 1972a, 1972b, Hanba et al. 1999, Warren et al. 2003, Koch et al. 2004).

Morphological changes with increasing height (e.g., higher SMA) decrease photosynthetic capacity (Figure 4D, Reich et al. 1997, Niinemets 1999), in part because higher respiration rates in denser tissues near the treetop reduce net photosynthesis (Figure 4B, Koch et al. 2004, Ishii et al. 2008). This relationship helps to explain observed increases in LCP within crowns and among treetops (Figure 4B and D). Compared to non-treetop foliage, treetop foliage has higher respiration rates, is acclimated to higher irradiance, and therefore requires more light to realize a net carbon gain (Lewis et al. 2000). Even in the presence of high light, increased respiratory costs coupled with reduced maximum photosynthetic rates in treetop foliage may severely reduce net carbon gain at great heights (Givnish et al. 2004). In contrast to treetop foliage, low-SMA foliage lower in the crown has low respiration rates and is capable of positive net photosynthesis in deep shade (Poorter 1999). Maximum photosynthesis and carbon gain are therefore attained at lower light levels in lower-crown foliage and reflected by lower LSP and LCP, respectively (Figures 4C and D).

Anatomical changes with increasing height also limit photosynthesis by inhibiting CO₂ conductance. Because the primary enzyme responsible for photosynthesis (Rubisco) has a low affinity for CO₂ and often operates at a fraction of its catalytic capacity, the CO₂ gradient within leaves affects photosynthetic efficiency (Evans and von Caemmerer 1996). Internal conductance from the substomatal chamber through the mesophyll regulates CO₂ concentration at carboxylation sites (Evans et al. 1986). As tissue density increases and intercellular airspaces diminish, the liquid phase of g_i becomes more limiting, constraining the amount of CO₂ reaching carboxylation sites (Hanba et al. 1999, Flexas et al. 2008), and lowering the amount of carbon gained relative to water lost in photosynthesis (Evans and von Caemmerer 1996). Even under optimal conditions, g_i can limit photosynthesis by 20% (Warren et al. 2003). Water stress further reduces g_i and curbs photosynthetic capacity (Niinemets 2007). Thus, g_i heavily influences photosynthetic water and nitrogen use efficiencies (PWUE and PNUE, respectively, Warren and Adams 2006). Along the height gradient in tall redwoods, PWUE increases but does not correlate with exponential increases in light availability indicating that photosynthetic efficiency in the upper crowns is not determined primarily by light availability (Ishii et al. 2008). Instead, photosynthetic efficiency in the upper crowns of tall redwoods is controlled by rates of mitochondrial respiration and internal CO₂ conductance related to tissue density.

Higher respiration and lower internal conductance are two costs associated with increasing height that limit net

photosynthesis near the tops of the tallest trees. Although the values reported here for internal conductance in redwoods are similar to those reported for other evergreen conifers (Flexas et al. 2008), confirmation of these values using a different method such as fluorescence is needed. Further investigation of how morphological constraints affect the plasticity of internal conductance is also warranted.

Acknowledgments

This work was funded by the National Science Foundation (IOB-0445277), the endowment creating the Kenneth L. Fisher Chair in Redwood Forest Ecology at Humboldt State University, and Global Forest Science. Comments from two anonymous reviewers greatly improved this manuscript.

References

- Ambrose, A.R., S.C. Sillett and T.E. Dawson. 2009. Effects of tree height on branch hydraulics, leaf structure, and gas exchange in California redwoods. *Plant Cell Environ.* (in press), doi: 10.1111/j.1365-3040.2009.01950.x.
- Bauerle, W.L., T.M. Hinckley, J. Cermak, J. Kucera and K. Bible. 1999. The canopy water relations of old-growth Douglas-fir trees. *Trees* 13:211–217.
- Bond, B.J., B.T. Farnsworth, R.A. Coulombe and W.E. Winner. 1999. Foliage physiology and biochemistry in response to light gradients in conifers with varying shade tolerance. *Oecologia* 120:183–192.
- Domec, J.C., B. Lachenbruch, F.C. Meinzer, D.R. Woodruff, J.M. Warren and K.A. McCulloh. 2008. Maximum height in a conifer is associated with conflicting requirements for xylem design. *Proc. Natl. Acad. Sci. USA* 105:12069–12074.
- Ethier, G.J. and N.J. Livingston. 2004. On the need to incorporate sensitivity to CO₂ transfer conductance into the Farquhar–von Caemmerer–Berry leaf photosynthesis model. *Plant Cell Environ.* 27:137–153.
- Evans, J.R. and S. von Caemmerer. 1996. Carbon dioxide diffusion inside leaves. *Plant Physiol.* 110:339–346.
- Evans, J.R., T.D. Sharkey, J.A. Berry and G.D. Farquhar. 1986. Carbon isotope discrimination measured concurrently with gas exchange to investigate CO₂ diffusion in leaves of higher plants. *Aust. J. Plant Physiol.* 13:281–292.
- Evans, J.R., S. von Caemmerer, B.A. Setchell and G.S. Hudson. 1994. The relationship between CO₂ transfer conductance and leaf anatomy in transgenic tobacco with a reduced content of Rubisco. *Aust. J. Plant Physiol.* 21:485–495.
- Flexas, J., M. Ribas-Carbo, A. Diaz-Espejo, J. Galmes and H. Medrano. 2008. Mesophyll conductance to CO₂: current knowledge and future prospects. *Plant Cell Environ.* 31: 602–621.
- Givnish, T.J. 1986. *On the economy of plant form and function.* Cambridge University Press, Cambridge, MA.
- Givnish, J.T., R.A. Montgomery and G. Goldstein. 2004. Adaptive radiation of photosynthetic physiology in the Hawaiian lobeliads: light regimes, static light responses, and whole-plant compensation points. *Am. J. Bot.* 91:228–246.
- Gorton, H.L., S.K. Herbert and T.C. Vogelmann. 2003. Photoacoustic analysis indicates that chloroplast movement does not alter liquid-phase CO₂ diffusion in leaves of *Alocasia brisbanensis*. *Plant Physiol.* 132:1529–1539.
- Griffin, K.L., D.T. Tissue, M.H. Turnbull, W. Schuster and D. Whitehead. 2001. Leaf dark respiration as a function of canopy position in *Nothofagus fusca* trees grown at ambient and elevated CO₂ partial pressures for 5 years. *Funct. Ecol.* 15:497–505.
- Hanba, Y.T., S.I. Miyazawa and I. Terashima. 1999. The influence of leaf thickness on the CO₂ transfer conductance and leaf stable carbon isotope ratio for some evergreen tree species in Japanese warm-temperate forests. *Funct. Ecol.* 13:632–639.
- Ishii, H.T., E.D. Ford, M.E. Boscolo, A.C. Manriquez, M.E. Wilson and T.M. Hinkley. 2002. Variation in specific needle area of old-growth Douglas-fir in relation to needle age, within-crown position and epicormic shoot production. *Tree Physiol.* 22:31–40.
- Ishii, H.T., G.M. Jennings, S.C. Sillett and G.W. Koch. 2008. Hydrostatic constraints on morphological exploitation of light in tall *Sequoia sempervirens* trees. *Oecologia* 156:751–763.
- Jennings, G.M. 2002. Vertical hydraulic gradients and the cause of foliar variation in tall redwood trees (*Sequoia sempervirens*). Thesis, Humboldt State University, Arcata, CA.
- Jepson, J. 2000. *The tree climber's companion.* Beaver Tree Publishing, Longville, MN.
- Jones, H.G. and R.O. Slatyer. 1972a. Effects of intercellular resistances on estimates of the intracellular resistance to CO₂ uptake by plant leaves. *Aust. J. Biol. Sci.* 25:443–453.
- Jones, H.G. and R.O. Slatyer. 1972b. Estimation of the transport and carboxylation components of the intracellular limitation to leaf photosynthesis. *Plant Physiol.* 50:283–288.
- Koch, G.W., S.C. Sillett, G.M. Jennings and S.D. Davis. 2004. The limits to tree height. *Nature* 428:851–854.
- Laisk, A. 1977. Kinetics of photosynthesis and photorespiration in C₃ plants. Nauka, Moscow, Russia (in Russian).
- Leverenz, J.W. 1996. Shade-shoot structure, photosynthetic performance in the field, and photosynthetic capacity of evergreen conifers. *Tree Physiol.* 16:109–114.
- Lewis, J.D., R.B. McKane, D.T. Tingey and P.A. Beedlow. 2000. Vertical gradients in photosynthetic light response within an old-growth Douglas-fir and western hemlock canopy. *Tree Physiol.* 7:447–456.
- Li, J., Y.M. Ou-Lee, R. Raba, R.G. Amundson and R.L. Last. 1993. *Arabidopsis* flavonoids mutants are hypersensitive to UV-B irradiation. *Plant Cell* 5:171–179.
- Marshall, J.D. and R.A. Monserud. 2003. Foliage height influences specific leaf area of three conifer species. *Can. J. For. Res.* 33:164–170.
- Maxwell, K., S. von Caemmerer and J.R. Evans. 1997. Is a low internal conductance to CO₂ diffusion a consequence of succulence in plants with Crassulacean Acid Metabolism? *Aust. J. Plant Physiol.* 24:777–786.
- McDowell, N.G., N. Phillips, C. Lurch, B.J. Bond and M.G. Ryan. 2002. An investigation of hydraulic limitation and compensation in large, old Douglas-fir trees. *Tree Physiol.* 22:763–774.
- Meinzer, F.C., B.J. Bond and J.A. Karanian. 2008. Biophysical constraints on leaf expansion in a tall conifer. *Tree Physiol.* 28:197–206.
- Mott, K.A., A.C. Gibson and J.W. O'Leary. 1982. The adaptive significance of amphistomatic leaves. *Plant Cell Environ.* 5:455–460.

- Niinemets, U. 1999. Research review: Components of leaf dry mass per area – thickness and density – alter leaf photosynthetic capacity in reverse directions in woody plants. *New Phytol.* 144:35–47.
- Niinemets, U. 2007. Photosynthesis and resource distribution through plant canopies. *Plant Cell Environ.* 30:1052–1071.
- Niinemets, U. and O. Kull. 1998. Stoichiometry of foliar carbon constituents varies along light gradients in temperate wood canopies: implications for foliage morphological plasticity. *Tree Physiol.* 18:467–479.
- Niinemets, U., O. Kull and J.D. Tenhunen. 1998. An analysis of light effects on foliar morphology, physiology, and light interception in temperate deciduous woody species of contrasting shade-tolerance. *Tree Physiol.* 18:681–696.
- Nobel, P.S. 1983. Biophysical plant physiology and ecology. W.H. Freeman & Co., San Francisco, CA.
- Norman, J.M. and T.J. Arkebauer. 1991. Predicting canopy light-use efficiency from leaf characteristics. *In* Modeling Plant Soil Systems. Eds. J.T. Ritchie and J. Hanks. American Society of Agronomy, Madison, WI, Agron Monograph 31.
- Oldham, A.R. 2008. Height-associated variation in leaf anatomy of tall redwoods: potential impacts on whole-tree carbon balance. Thesis, Humboldt State University, Arcata, CA.
- Peisker, M. and H. Apel. 2001. Inhibition by light of CO₂ evolution from dark respiration: comparison of two gas exchange methods. *Photosynth. Res.* 70:291–298.
- Phillips, N.G., M.G. Ryan, B.J. Bond, N.G. McDowell, T.M. Hinckley and J. Cermak. 2003. Reliance on stored water increases with tree size in three species in the Pacific Northwest. *Tree Physiol.* 23:237–245.
- Poorter, L. 1999. Growth responses of 15 rain-forest tree species to a light gradient: the relative importance of morphological and physiological traits. *Funct. Ecol.* 13:396–410.
- Poorter, H., S. Pepin, T. Rijkers, Y. de Jong, J.R. Evans and C. Korner. 2006. Construction costs, chemical composition and payback time of high- and low-irradiance leaves. *J. Exp. Bot.* 57:355–371.
- Poorter, H., U. Niinemets, L. Poorter, I.J. Wright and R. Villar. 2009. Causes and consequences of variation in leaf mass per area (LMA): a meta-analysis. *New Phytol.* 182:565–588.
- Reich, P.B., M.B. Walters and D.S. Ellsworth. 1997. From tropics to tundra: global convergence in plant functioning. *Proc. Natl. Acad. Sci. USA* 94:13730–13734.
- Reich, P.B., D.S. Ellsworth, M.B. Walters, J.M. Vose, C. Gresham, J.C. Volin and W.D. Bowman. 1999. Generality of leaf trait relationships: a test across six biomes. *Ecology* 80:1955–1969.
- Ryan, M.G. and B.J. Yoder. 1997. Hydraulic limits to tree height and growth. *BioScience* 47:235–242.
- Ryan, M.G., N. Phillips and B.J. Bond. 2006. The hydraulic limitation hypothesis revisited. *Plant Cell Environ.* 29:367–381.
- Sharkey, T.D., C.J. Bernacchi, G.D. Farquhar and E.L. Singaas. 2007. Fitting photosynthetic carbon dioxide response curves for C₃ leaves. *Plant Cell Environ.* 30:1035–1040.
- Syvrtsen, J.P., J. Lloyd, C. McConchie, P.E. Kriedemann and G.D. Farquhar. 1995. On the relationship between leaf anatomy and CO₂ diffusion through the mesophyll of hypostomatous leaves. *Plant Cell Environ.* 18:149–157.
- Teeri, J.A., S.J. Tonsor and M. Turner. 1981. Leaf thickness and carbon isotope composition in the Crassulaceae. *Oecologia* 50:367–369.
- Tissue, D.T., J.D. Lewis, S.D. Wullschlegel, J.S. Amthor, K.L. Griffin and O.R. Anderson. 2002. Leaf respiration at different canopy positions in sweetgum (*Liquidambar styraciflua*) grown in ambient and elevated concentrations of carbon dioxide in the field. *Tree Physiol.* 22:1157–1166.
- Van Pelt, R. and J.F. Franklin. 2000. Influence of canopy structure on the understory environment in tall, old-growth, conifer forest. *Can. J. For. Res.* 30:1231–1245.
- von Caemmerer, S. and J.R. Evans. 1991. Determination of the average partial pressure of CO₂ in chloroplasts from leaves of several C₃ plants. *Aust. J. Plant Physiol.* 18:287–305.
- Warren, C.R. 2008. Stand aside stomata, another actor deserves centre stage: the forgotten role of the internal conductance to CO₂ transfer. *J. Exp. Bot.* 59:1475–1487.
- Warren, C.R. and M.A. Adams. 2006. Internal conductance does not scale with photosynthetic capacity: implications for carbon isotope discrimination and the economics of water and nitrogen use in photosynthesis. *Plant Cell Environ.* 29:192–201.
- Warren, C.R., G.J. Ethier, N.J. Livingston, N.J. Grant, D.H. Turpin, D.L. Harrison and T.A. Black. 2003. Transfer conductance in second growth Douglas-fir (*Pseudotsuga menziesii* (Mirb.) Franco) canopies. *Plant Cell Environ.* 26:1215–1227.
- Warren, C.R., N.J. Livingston and D.H. Turpin. 2004. Water stress decreases the transfer conductance of Douglas-fir (*Pseudotsuga menziesii*) seedlings. *Tree Physiol.* 24:971–979.
- Woodruff, D.R., B.J. Bond and F.C. Meinzer. 2004. Does turgor limit growth in tall trees? *Plant Cell Environ.* 27:229–236.
- Woodruff, D.R., F.C. Meinzer, B. Lachenbruch and D.M. Johnson. 2008. Coordination of leaf structure and gas exchange along a height gradient in a tall conifer. *Tree Physiol.* 29:261–272.
- Zha, T., K. Wang, A. Ryyppo and S. Kellomaki. 2002. Needle dark respiration in relation to within-crown position in Scots pine trees grown in long-term elevation of CO₂ concentration and temperature. *New Phytol.* 156:33–41.
- Zimmermann, M.H. 1971. Tree structure and function. Springer-Verlag, New York.
- Zimmermann, M.H. 1983. Xylem structure and the ascent of sap. Springer-Verlag, Berlin.

Appendix

Table A1. Summary of terms and definitions used in this study.

Abbreviation	Definition	Unit
$A_{\max,a}$	Area-based maximum CO ₂ assimilation rate	$\mu\text{mol CO}_2 \text{ m}^{-2} \text{ s}^{-1}$
$A_{\max,m}$	Mass-based maximum CO ₂ assimilation rate	$\text{nmol CO}_2 \text{ g}^{-1} \text{ s}^{-1}$
$A_{\text{std},a}$	Area-based standardized CO ₂ assimilation rate	$\mu\text{mol CO}_2 \text{ m}^{-2} \text{ s}^{-1}$
$A_{\text{std},m}$	Mass-based standardized CO ₂ assimilation rate	$\text{nmol CO}_2 \text{ g}^{-1} \text{ s}^{-1}$
A_s	Projected shoot area	cm^2
C_i	Internal CO ₂ concentration in substomatal chamber	$\mu\text{mol CO}_2 \text{ mol}^{-1}$
C_i^*	Intercellular CO ₂ compensation point	$\mu\text{mol CO}_2 \text{ mol}^{-1}$
$g_{i,a}$	Area-based internal conductance of CO ₂	$\text{mol CO}_2 \text{ m}^{-2} \text{ s}^{-1} \text{ bar}^{-1}$
$g_{i,m}$	Mass-based internal conductance of CO ₂	$\text{nmol CO}_2 \text{ g}^{-1} \text{ s}^{-1} \text{ bar}^{-1}$
g_{ias}	Internal CO ₂ conductance through intercellular airspaces	$\text{mol CO}_2 \text{ m}^{-2} \text{ s}^{-1} \text{ bar}^{-1}$
g_{liq}	Internal CO ₂ conductance through mesophyll cells	$\text{mol CO}_2 \text{ m}^{-2} \text{ s}^{-1} \text{ bar}^{-1}$
$g_{s,a}$	Area-based stomatal conductance of CO ₂	$\text{mol CO}_2 \text{ m}^{-2} \text{ s}^{-1} \text{ bar}^{-1}$
$g_{s,m}$	Mass-based stomatal conductance of CO ₂	$\text{nmol CO}_2 \text{ g}^{-1} \text{ s}^{-1} \text{ bar}^{-1}$
M_r	Molecular weight	g mol^{-1}
M_s	Shoot dry weight	g
LCP	Light compensation point	$\mu\text{mol photons m}^{-2} \text{ s}^{-1}$
LMA	Leaf mass-to-area ratio	g m^{-2}
LSP	Light saturation point	$\mu\text{mol photons m}^{-2} \text{ s}^{-1}$
PNUE	Photosynthetic nitrogen use efficiency	$\text{nmol CO}_2 \text{ mol H}_2\text{O}^{-1}$
PPFD	Photosynthetic photon flux density	$\mu\text{mol photons m}^{-2} \text{ s}^{-1}$
PWUE	Photosynthetic water use efficiency	$\mu\text{mol CO}_2 \text{ mol}^{-1} \text{ s}^{-1}$
R_d	Day respiration rate	$\mu\text{mol CO}_2 \text{ m}^{-2} \text{ s}^{-1}$
$R_{m,a}$	Area-based mitochondrial (dark) respiration	$\mu\text{mol CO}_2 \text{ m}^{-2} \text{ s}^{-1}$
$R_{m,m}$	Mass-based mitochondrial (dark) respiration	$\text{nmol CO}_2 \text{ g}^{-1} \text{ s}^{-1}$
SMA	Shoot mass-to-area ratio	g m^{-2}
$\delta^{13}\text{C}$	Ratio of stable isotopes ¹³ C: ¹² C	‰
Γ^*	Photocompensation point	$\mu\text{mol mol}^{-1}$